



Royal Netherlands Institute for Sea Research

This is a postprint of:

Ballesta-Artero, I.; Zhao, L.; Milano, S.; Mertz-Kraus, R.;
Schöne, B.R.; van der Meer, J. & Witbaard, R. (2018).
Environmental and biological factors influencing trace elemental
and microstructural properties of *Arctica islandica* shells.
Science of the Total Environment, 645, 913-923

Published version: <https://doi.org/10.1016/j.scitotenv.2018.07.116>

Link NIOZ Repository: <http://www.vliz.be/imis?module=ref&refid=301843>

[Article begins on next page]

The NIOZ Repository gives free access to the digital collection of the work of the Royal Netherlands Institute for Sea Research. This archive is managed according to the principles of the [Open Access Movement](#), and the [Open Archive Initiative](#). Each publication should be cited to its original source - please use the reference as presented.

When using parts of, or whole publications in your own work, permission from the author(s) or copyright holder(s) is always needed.

1 **Environmental and biological factors influencing trace elemental and**
2 **microstructural properties of *Arctica islandica* shells**

3 Irene Ballesta-Artero ^{a,b,c}, Liqiang Zhao ^{d,e}, Stefania Milano ^{d,f}, Regina Mertz-Kraus ^d; Bernd R. Schöne ^d,
4 Jaap van der Meer ^{a,c}, Rob Witbaard ^b

5
6 ^a NIOZ; Netherlands Institute for Sea Research and Utrecht University, Department of Coastal Systems, PO Box 59,
7 1790 AB Den Burg, Texel, The Netherlands

8 ^b NIOZ; Netherlands Institute for Sea Research and Utrecht University, Department of Estuarine and Delta Systems,
9 PO Box 140, 4400 AC Yerseke, The Netherlands

10 ^c Department of Animal Ecology, VU University Amsterdam, The Netherlands

11 ^d Institute of Geosciences, University of Mainz, Joh.-J.-Becher-Weg 21, 55128 Mainz, Germany

12 ^e Department of Atmosphere and Ocean Research Institute, University of Tokio, Japan (Present address)

13 ^f Department of Human Evolution, Max Planck Institute for Evolutionary Anthropology, Leipzig, Germany (Present
14 address)

15

16 * *corresponding author: irene.ballesta.artero@nioz.nl (Irene Ballesta-Artero)*

17

18 Long-term and high-resolution environmental proxy data are crucial to contextualize current
19 climate change. The extremely long-lived bivalve, *Arctica islandica*, is one of the most widely used
20 paleoclimate archives of the northern Atlantic because of its fine temporal resolution. However,
21 the interpretation of environmental histories from microstructures and elemental impurities of *A.*
22 *islandica* shells is still a challenge. Vital effects (metabolic rate, ontogenetic age, and growth rate)
23 can modify the way in which physiochemical changes of the ambient environment are recorded by
24 the shells. To quantify the degree to which microstructural properties and element incorporation
25 into *A. islandica* shells is vitally or/and environmentally affected, *A. islandica* specimens were

26 reared for three months under different water temperatures (3, 8 and 13 °C) and food concentrations
27 (low, medium and high). Concentrations of Mg, Sr, Na, and Ba were measured in the newly formed
28 shell portions by laser ablation-inductively coupled plasma-mass spectrometry (LA-ICP-MS). The
29 microstructures of the shells were analyzed by Scanning Electron Microscopy (SEM). Shell growth
30 and condition index of each specimen were calculated at the end of the experimental period.

31 Findings indicate that no significant variation in the morphometric characteristics of the
32 microstructures were formed at different water temperatures or different food concentrations. Shell
33 carbonate that formed at lowest food concentration usually incorporated the highest amounts of
34 Mg, Sr and Ba relative to Ca^{+2} (except for Na) and was consistent with the slowest shell growth
35 and lowest condition index at the end of the experiment. These results seem to indicate that, under
36 food limitation, the ability of *A. islandica* to discriminate element impurities during shell formation
37 decreases. Moreover, all trace element-to-calcium ratios were significantly affected by shell growth
38 rate. Therefore, physiological processes seem to dominate the control on element incorporation
39 into *A. islandica* shells.

40

41 **Keywords:**

42 Bivalve, environmental proxy, vital effects, temperature, phytoplankton concentration,
43 sclerochronology

44

45 **1. Introduction**

46 Proxy records are crucial to study climate change in areas where instrumental records are absent
47 (Freitas et al., 2006). In the last two decades, bivalve shells have become an important bioarchive
48 tool and the number of respective studies has greatly increased (Gillikin et al., 2005; Freitas et al.,
49 2006; Wanamaker et al., 2008; Schöne et al., 2011; Milano et al., 2017a). Microstructural
50 properties and trace element-to-calcium ratios can reflect the environment in which the bivalves
51 lived (Schöne et al., 2013; Milano et al., 2017a). The long-living species *Arctica islandica* (up to
52 507 years old; Wanamaker et al., 2008, Butler et al., 2013), also known as ocean quahog, has been
53 widely used for multicentennial paleoclimatic reconstruction (Butler et al., 2013), but the study of
54 its microstructural and geochemical shell properties as an environmental proxy is still under
55 development. Therefore, knowledge of the interacting effects of extrinsic (environmental) and
56 intrinsic (physiological) factors on *A. islandica* shells are essential to interpret this long-living
57 bioarchive (Abele et al., 2009).

58 Levels of strontium (Sr) and magnesium (Mg) in bivalve shells have been proposed as proxies
59 for water temperature (Klein et al., 1996; Schöne et al., 2013). However, Sr/Ca and Mg/Ca ratios
60 are still difficult to interpret because the incorporation of trace and minor impurities in the shell
61 carbonate is partly physiologically controlled (e.g., Urey et al., 1951; Purton et al., 1999; Lorrain
62 et al., 2005; Freitas et al., 2005, 2006; Schöne et al., 2010, 2013; Marali et al., 2017a; Geeza et
63 al., 2018). Published results on the relationship between the Sr/Ca and Mg/Ca ratios of bivalve
64 shells and temperature are highly ambiguous; previous studies have reported a positive
65 relationship (Stecher et al., 1996; Hart and Blusztajn, 1998; Toland et al., 2000), negative
66 relationship (Dodd, 1965; Stecher et al., 1996; Surge and Walker, 2006; Schöne et al., 2011), and
67 no relationship (Gillikin et al., 2005; Strasser et al., 2008; Izumida et al., 2011; Wanamaker and

68 Gillikin, 2018). The variation on the type of relationship (positive, negative, or neutral) have been
69 identified as species-specific and can even change depending on the season of the year (e.g.,
70 Gillikin et al., 2005; Freitas et al., 2006). In addition, Sr/Ca and Mg/Ca ratios can even differ
71 among specimens of the same population, but the causes are not yet clear (Vander Putten et al.,
72 2000; Lorrain et al., 2005; Freitas et al., 2006; Foster et al., 2008, 2009).

73 The potential use of other element-to-calcium ratios of bivalve shells as environmental proxies
74 has also been explored. For example, Na/Ca is strongly correlated to salinity (Rucker and
75 Valentine, 1961; O'Neil and Gillikin, 2014) and water pH (Zhao et al., 2017a). Furthermore, it
76 has been suggested that Ba/Ca and Na/Ca ratios are linked to primary production (e.g., Stecher et
77 al., 1996; Gillikin et al., 2006; Poulain et al., 2015; Klünder et al., 2008). Ba/Ca profiles are
78 typically characterized by a relatively flat background interrupted by episodic sharp peaks (e.g.,
79 Stecher et al., 1996; Vander Putten et al., 2000; Gillikin et al., 2006, 2008; Thébault et al., 2009;
80 Elliot et al., 2009; Hatch et al., 2013), which are usually highly reproducible among specimens
81 (e.g., Gillikin et al., 2008; Elliot et al., 2009; Marali et al., 2017a, b). Although the factors
82 controlling the formation of Ba/Ca peaks are still controversially debated, the Ba/Ca ratio of
83 bivalve shells is potentially strongly influenced by an environmental forcing (Gillikin et al., 2006,
84 2008; Poulain et al., 2015).

85 Previous studies of mollusks show that environmental parameters can also influence the
86 microstructure of the shell (Lutz, 1984; Tan Tiu and Prezant, 1987; Tan Tiu, 1988; Nishida et al.,
87 2012) and therefore, can serve as potential proxy for environmental conditions (Tan Tiu, 1988;
88 Tan Tiu and Prezant, 1989; Schöne et al., 2010; Milano et al., 2017b). For example, the size and
89 elongation of individual biominerals in *Cerastoderma edule* (Milano et al., 2017b) and the
90 cyclical changes in thickness of the outer layer of *Scapharca broughtonii* (Nishida et al., 2012)

91 shells are related to temperature changes. Moreover, the relationship between food conditions and
92 microstructure have lately been explored; some studies reported an accumulation of pigments in
93 mollusk shells due to the ingestion of pigment-enriched microalgae (polyenes; Hedegaard et al.
94 2006; Soldatov et al., 2013), while others argued that diets do not influence shell pigment
95 composition, and that polyenes are likely species-specific and habitat independent (Nehrke and
96 Nouet, 2011; Stemmer and Nehrke, 2014; Milano et al., 2017a). The study of shell microstructure
97 can therefore help to develop alternative techniques to reconstruct environmental variables from
98 bivalve shells (Milano et al., 2017a).

99 The objective of the present study is to clarify the effect of external (environmental) and
100 internal (physiological) factors on microstructural properties and element incorporation into *A.*
101 *islandica* shells. Under laboratory conditions, *A. islandica* individuals from the same population
102 were reared at different temperatures and food concentrations. Several studies have used
103 controlled laboratory experiments to determine the relationship between the elemental
104 composition of bivalve shells and variable environmental parameters (Lorens and Bender, 1980;
105 Strasser et al., 2008; Wanamaker et al., 2008; Poulain et al., 2015; Wanamaker and Gillikin,
106 2018). However, fewer studies have tested the effect of the environment on the shell
107 microstructure. Furthermore, most previous studies only focused on single parameter validation
108 and did not take into account the possible interaction among multiple parameters (e.g., Lorens
109 and Bender, 1980; Poulain et al., 2015). Here, we present for the first time a controlled laboratory
110 experiment that aim to provide a better understanding of the interplay between environmental
111 (food and temperature) and physiological influence (shell growth and condition index) on the
112 geochemical properties and shell microstructure of *A. islandica* shells.

113

114 **2. Materials and methods**

115 *2.1. Sample collection*

116 In July 2014, live juvenile specimens of *A. islandica* were collected from the Kiel Bay, Baltic Sea
117 (54° 32' N, 10° 42' E) and used in a laboratory growth experiment conducted at Royal
118 Netherlands Institute for Sea Research (NIOZ) between 22 March and 23 June 2016 (14 weeks;
119 Ballesta-Artero et al., 2018). The specimens were divided among 12 different treatments, i.e.,
120 combinations of four food concentrations (no, low, medium, and high food) and three different
121 temperatures (3 °C, 8 °C, and 13 °C; Table 1). There were 3 replicates per treatment (3 aquaria),
122 which meant a total of 36 aquaria (4 food levels x 3 temperatures x 3 replicates). Five *A.*
123 *islandica* juveniles were randomly assigned to each aquarium, amounting to a total 180 *A.*
124 *islandica* specimens. Specimens reared without food were not analyzed in this study because
125 there was insufficient (or none) newly formed shell material for chemical analyses (Ballesta-
126 Artero et al., 2018). Therefore, we only analyzed 9 treatments (27 trials) and a total of 73
127 specimens for the present study. Bivalves were fed 8 times per day with a commercial mix of
128 marine microalgae containing *Isochrysis* sp., *Tetraselmis* sp., *Pavlova* sp., *Thalassiosira* sp. and
129 *Nannochloropsis* spp (Mixalgae; Acuinuga, Spain). Numbers of cells in each aquarium were
130 checked once per week with a flow cytometer (BD Accuri C6), while temperature and salinity
131 were monitored on a daily basis with a portable multiparameter probe (HI98192; Hanna
132 instruments, USA).

133 The starting shell height of the experimental animals ranged between 8.31 and 14.34 mm (\pm
134 0.01 mm). Prior to the start of the experiment, the specimens were soaked in a calcein solution of
135 125mg/l for 24 hours (Linard et al., 2011; Ambrose et al., 2012). This solution allowed us to
136 accurately identify the newly formed shell portion that grew under experimental conditions.

	3 °C	8 °C	13 °C
Low			
Na/Ca	23.94 ± 0.70	23.27 ± 0.75	23.58 ± 1.39
Mg/Ca	0.44 ± 0.05	0.40 ± 0.02	0.47 ± 0.08
Sr/Ca	1.58 ± 0.17	1.49 ± 0.06	1.68 ± 0.17
Ba/Ca	8.48 ± 2.78	8.27 ± 1.26	8.32 ± 3.75
Condition Index	5.27 ± 0.21	3.72 ± 0.57	4.33 ± 0.37
Shell growth	0.40 ± 0.28	0.28 ± 0.22	0.39 ± 0.44
[cells/ L] x 10 ⁶	0.85 ± 0.43	0.22 ± 0.02	0.53 ± 0.18
mg DW /ind/ d	0.62 ± 0.01	0.62 ± 0.01	0.62 ± 0.01
Medium			
Na/Ca	25.42 ± 1.54	24.99 ± 0.40	24.25 ± 1.45
Mg/Ca	0.38 ± 0.14	0.32 ± 0.06	0.36 ± 0.02
Sr/Ca	1.55 ± 0.21	1.43 ± 0.06	1.50 ± 0.04
Ba/Ca	9.56 ± 7.18	11.84 ± 6.84	5.26 ± 1.69
Condition Index	7.83 ± 0.22	5.59 ± 0.57	6.92 ± 0.96
Shell growth	0.90 ± 0.24	1.65 ± 0.35	1.82 ± 0.52
[cells/ L] x 10 ⁶	6.19 ± 0.64	2.34 ± 0.17	1.53 ± 0.05
mg DW /ind/ d	5.33 ± 0.21	5.33 ± 0.21	5.33 ± 0.21
High			
Na/Ca	25.98 ± 2.08	24.79 ± 0.23	23.95 ± 0.76
Mg/Ca	0.43 ± 0.17	0.31 ± 0.04	0.35 ± 0.11
Sr/Ca	1.41 ± 0.17	1.42 ± 0.09	1.75 ± 0.10
Ba/Ca	6.29 ± 3.56	7.17 ± 0.48	5.86 ± 1.91
Condition Index	7.62 ± 2.64	9.01 ± 2.13	9.24 ± 1.02
Shell growth	0.72 ± 0.39	1.34 ± 0.40	1.48 ± 0.05
[cells/ L] x 10 ⁶	24.56 ± 2.85	12.99 ± 0.82	6.45 ± 2.08
mg DW /ind/ d	13.69 ± 0.03	13.69 ± 0.03	13.69 ± 0.03
T real (°C)	2.49 ± 0.02	7.94 ± 0.07	13.11 ± 0.05
Salinity(PPT)	30.26 ± 0.10	30.38 ± 0.08	29.39 ± 0.24

138 **Table 1:** Summary of treatments (mean ± SD). Results are given in µm/mol for Ba/Ca and
139 mmol/mol for the other elements. Shell growth was measured in height (mm). DW= Dry weight
140 and ind= individual.

141

142

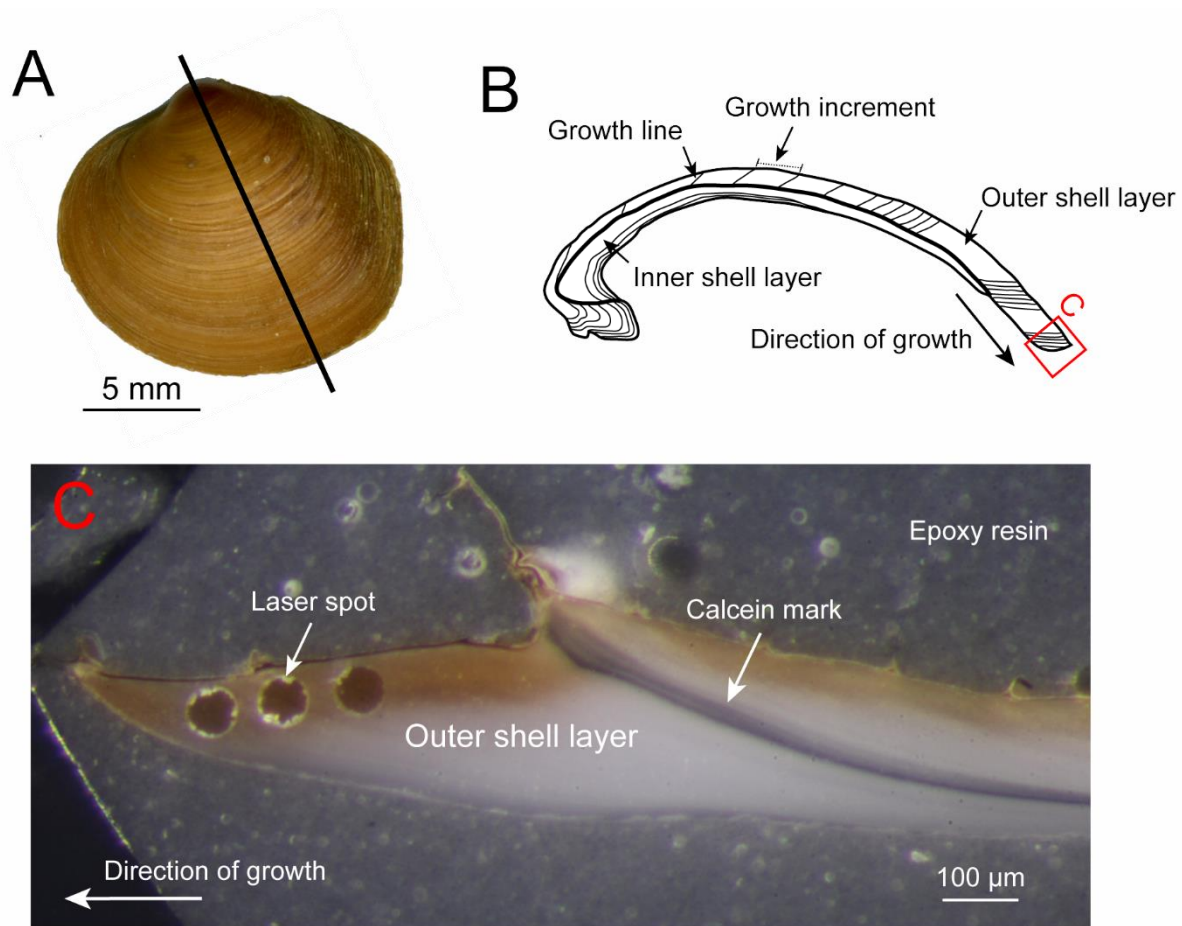
143 2.2. *Shell preparation*

144 The right valve of each specimen was glued to a plexiglass cube, covered with a layer of JB
145 KWIK epoxy resin and dried overnight. A low speed saw (Buehler IsoMet 1000; 250 rpm) was
146 used to cut 3-mm-thick section from each specimen along the axis of maximum growth.
147 Subsequently, the slabs were embedded in Struers EpoFix resin and air-dried overnight. The
148 blocks were then ground using Buehler silicon carbide papers of different grit sizes (P320, P600,
149 P1200, P2500) mounted on a Buehler Metaserv 2000 grinder-polisher machine. After each
150 grinding step the blocks were rinsed in an ultrasonic bath for ca. 2 min. The samples were
151 polished with a Buehler diamond polycrystalline suspension (3 μm) and rinsed once more. Prior
152 to the analyses, shell sections were examined under a fluorescence light stereomicroscope (Zeiss
153 AxioImager A1m fluorescent microscope equipped with a Zeiss HBO 100 mercury lamp for UV
154 light, and Zeiss filter set 18 with an excitation wavelength of ~450-500 nm and an emission
155 wavelength of ~500-550 nm), which clearly highlighted the calcein marks, indicating the newly
156 formed shell portion. Photographs were taken using a Canon EOS 600D digital camera connected
157 to the microscope. Newly formed increment widths (total growth over 14 weeks) were measured
158 using the free image processing software, ImageJ (National Institutes of Health, USA).

159

160 2. 3. *Laser Ablation-Inductively Coupled Plasma-Mass Spectrometry (LA-ICP-MS)*

161 Element concentrations of sodium (measured as ^{23}Na), magnesium (^{25}Mg), strontium (^{86}Sr) and
162 barium (^{137}Ba) were determined in 73 *A. islandica* shells (9 ± 2 specimens per treatment) at the
163 Institute of Geosciences, University of Mainz. We used an Agilent 7500ce inductively coupled
164 plasma-mass spectrometer (ICP-MS) coupled to an ESI NWR193 ArF excimer laser ablation
165 (LA) system which was equipped with a TwoVol² ablation cell.



166
 167 **Fig. 1:** Shell of juvenile *Arctica islandica* A) outer shell surface with line of maximum growth
 168 (black line) B) cross-sectioned shell with major structures C) magnification of the outer shell
 169 margin revealing calcein mark and laser spots.

170
 171 The ArF LA system was operated at a pulse repetition rate of 10 Hz, an energy density of
 172 $\sim 3 \text{ J/cm}^2$, and an ablation spot diameter of $55 \mu\text{m}$. Background measurement were performed for
 173 20 s, followed by ablation times of 40 s, and wash out times of 20 s. Ablation was carried out
 174 under a He atmosphere and the sample gas was mixed with Ar before entering the plasma. For
 175 each shell, measurements were performed at three equidistant spots in the middle of the aragonite
 176 layer of the newly formed shell portion (Fig. 1). The multi-element synthetic glass NIST SRM
 177 610 was used as calibration material, applying as the “true” concentrations the preferred values

178 reported in the GeoReM database (<http://georem.mpch-mainz.gwdg.de/>; Jochum et al., 2005,
179 2011). For all materials, ^{43}Ca was used as internal standard. For the reference materials, we
180 applied the Ca concentrations reported in the GeoReM database, and for the samples 56.03 wt.%,
181 the stoichiometric CaO content of CaCO_3 . During each analytical session, we analyzed
182 homogeneous basaltic USGS BCR-2G and synthetic carbonate USGS MACS-3 as quality control
183 materials (QCMs). Reproducibility, which was expressed as the relative standard deviation based
184 on repeated measurements of the QCM, was always better than 1.6 % for USGS BCR-2G ($n = 9$)
185 and 7.5 % for MACS-3 ($n = 9$). The measured Na, Mg, Sr, and Ba concentrations of USGS BCR-
186 2G agree within 1.4 %, 12.5 %, 2.1 %, and 0.5 % with the preferred values of the GeoReM
187 database and within 1.1 %, 5.0 %, 0.6 %, and 0.7 % with the preliminary reference values for
188 USGS MACS-3 (personal communication S. Wilson, USGS; Jochum et al., 2012). In the
189 following, the average of the element concentrations (of the three spots measurements) are
190 reported relative to Ca in mmol/mol for Sr, Mg and Na, and $\mu\text{mol/mol}$ for Ba.

191

192 *2.4. Shell microstructure*

193 *A. islandica* produces a shell composed of a single calcium carbonate polymorph (aragonite)
194 organized in layers characterized by different microstructures (Milano et al., 2017a). The outer
195 portion of the outer shell layer (oOSL) consists of homogenous microstructure, whereas the inner
196 portion of the outer shell layer (iOSL) and the inner shell layer (ISL) are dominated by crossed-
197 acicular microstructures (Dunca et al., 2009; Schöne et al., 2013; Milano et al., 2017a). The
198 homogenous microstructure is characterized by granular biomineral units distributed without a
199 specific structural arrangement (Carter et al., 2012). The crossed-acicular microstructure contains
200 elongated biomineral units obliquely aligned. The present study focuses on the ventral margin of

201 the shells outside the pallial line. In this area, the ISL is missing. SEM analyses were carried out
202 in the iOSL which has been previously identified as being potentially sensitive to environmental
203 changes in *Cerastoderma edule* (Milano et al., 2017b).

204 The microstructure of 32 *A. islandica* shells was analyzed using a Scanning Electron
205 Microscope (SEM). On average, four specimens were investigated per treatment (4 ± 2). The
206 selection of specimens was based on the amount of aragonite deposited during the experimental
207 phase. Shells with limited or no growth were omitted from the analysis. To study the
208 microstructures, samples were etched in 1 vol% HCl for 10 s and bleached in 6 vol% NaClO for
209 30 min. After being dried from air, the samples were coated with a 2 nm-thick platinum layer by
210 using a sputter coater (Leica EM ACE200). The microstructures were qualitatively analyzed with
211 a scanning electron microscope (LOT Quantum Design 2nd generation Phenom Pro desktop
212 SEM) with backscattered electron detector and 10kV accelerating voltage. SEM images were
213 taken over 100 μm away from the calcein line to avoid bias associated with the marking stress. In
214 each specimen, the SEM images represent an area of ca. 2 mm² located in the middle of the shell
215 portion formed during the experiment. In specimens with a large amount of aragonite deposited
216 during the experiment, a second area was selected for SEM analysis ca. 300 μm away from the
217 first area.

218

219 2.5. Shell growth

220 Shell growth was measured as the width between the ventral (outer) edge and the calcein mark
221 that had formed at the start of the experimental period (mm; 93 days). In this study, shell growth
222 is analogous to growth rate as all shells were grown over the same length of period.

223 2.6. *Condition Index*

224 Condition index (CI = dry soft tissue mass/ dry shell mass) of each specimen was calculated at
225 the end of the experimental period as a measure of their physiological state at the end of the
226 experiment. Dry weight was determined after drying the soft tissue at 60 °C for 3 days.

227

228 2.7. *Statistical analysis*

229 Experimental data were analyzed with R version 3.2.2. Since individual specimens within one
230 experimental unit (aquarium) were interdependent pseudo-replicates, we calculated single
231 average values for trace elements, condition index, and shell growth for each aquarium. Then,
232 data were checked for normality (Shapiro–Wilk’s test; $p < 0.05$) and homogeneity of variance
233 (Levene’s F -test ; $p < 0.05$) before applying a two-way analysis of variance (ANOVA). ANOVA
234 was used to test for significant effects among the different food-temperature treatments. Ba/Ca
235 and Mg/Ca ratios were log-transformed to follow ANOVA assumptions.

236 Univariate relationships between the average Na/Ca, Mg/Ca, Sr/Ca and Ba/Ca ratios of *A.*
237 *islandica* shells per aquarium, environmental parameters (temperature and food), shell growth,
238 and condition index were estimated by means of Pearson correlation analysis. Statistically
239 significant differences were set at a $p < 0.05$.

240

Variable response	Effect	df	Sum Sq	Mean Sq	F-value	Pr (> F)
Na/Ca	Food (F)	2	8.6698	4.3344	3.0953	0.0699
	Temperature (T)	2	7.3328	3.6664	2.6182	0.1004
	Interaction F*T	4	2.2196	0.5549	0.3963	0.8087
	Residuals	18	25.2060	1.4003		
log(Mg/Ca)	Food	2	0.0558	0.0279	2.9061	0.0806
	Temperature	2	0.0242	0.0121	1.2607	0.3073
	Interaction F*T	4	0.0115	0.0029	0.2996	0.8743
	Residuals	18	0.1728	0.0096		
Sr/Ca	Food	2	0.0367	0.0183	1.0657	0.3652
	<i>Temperature</i>	2	0.1862	0.0931	5.4131	0.0144
	Interaction F*T	4	0.1174	0.0294	1.7066	0.1924
	Residuals	18	0.3096	0.0172		
log(Ba/Ca)	Food	2	0.0656	0.03281	0.9155	0.4182
	Temperature	2	0.1060	0.05298	1.4781	0.2545
	Interaction F*T	4	0.0769	0.01923	0.5366	0.7107
	Residuals	18	0.6451	0.03584		
CI	<i>Food</i>	2	79.0870	39.5430	24.8314	6.67E-06
	Temperature	2	3.5250	1.7630	1.1069	0.3521
	Interaction F*T	4	12.3600	3.0900	1.9403	0.1473
	Residuals	18	28.6650	1.5920		
GH	<i>Food</i>	2	5.4311	2.7155	22.0637	2.52E-05
	<i>Temperature</i>	2	1.4654	0.7327	5.9530	0.0117
	Interaction F*T	4	0.8693	0.2173	1.7658	0.1851
	Residuals	16	1.9692	0.1231		

242

243 **Table 2:** Two-way ANOVA test on the effects of temperature and food level over the different
244 response variables (n=27, 27 trials). Significant factors per model are highlighted in italic. CI =
245 condition index, GH = shell growth in height.

246 Finally, a multi-regression analysis was performed with all the individual data to identify
247 which factor/s (temperature, food, shell growth, and electric conductivity: EC) were
248 mathematically linked to the trace element content of the shells using the following equation:

$$249 \quad y_i = \beta_0 + \beta_1 \times Temperature_i + \beta_2 \times Food_i + \beta_3 \times Shell\ growth_i + \beta_4 \times EC_i + \varepsilon_i$$

250 Where y_i was the trace element-to-calcium ratio of specimen i (i range 1–73), β_0 was the
251 intercept, β_{1-4} were the estimated coefficients of the different explanatory variables
252 (temperature, food concentration, shell growth, and EC, respectively), and ε_i was the model error
253 for each specimen ($\varepsilon_i \sim N(0,1)$). To avoid collinearity, explanatory variables were included in the
254 analyses only when they had a (Pearson) correlation coefficient $\leq \pm 0.5$ (Graham 2003; Duncan
255 2011; Ieno and Zuur 2015).

256 **3. Results**

257 *3.1. Experimental conditions*

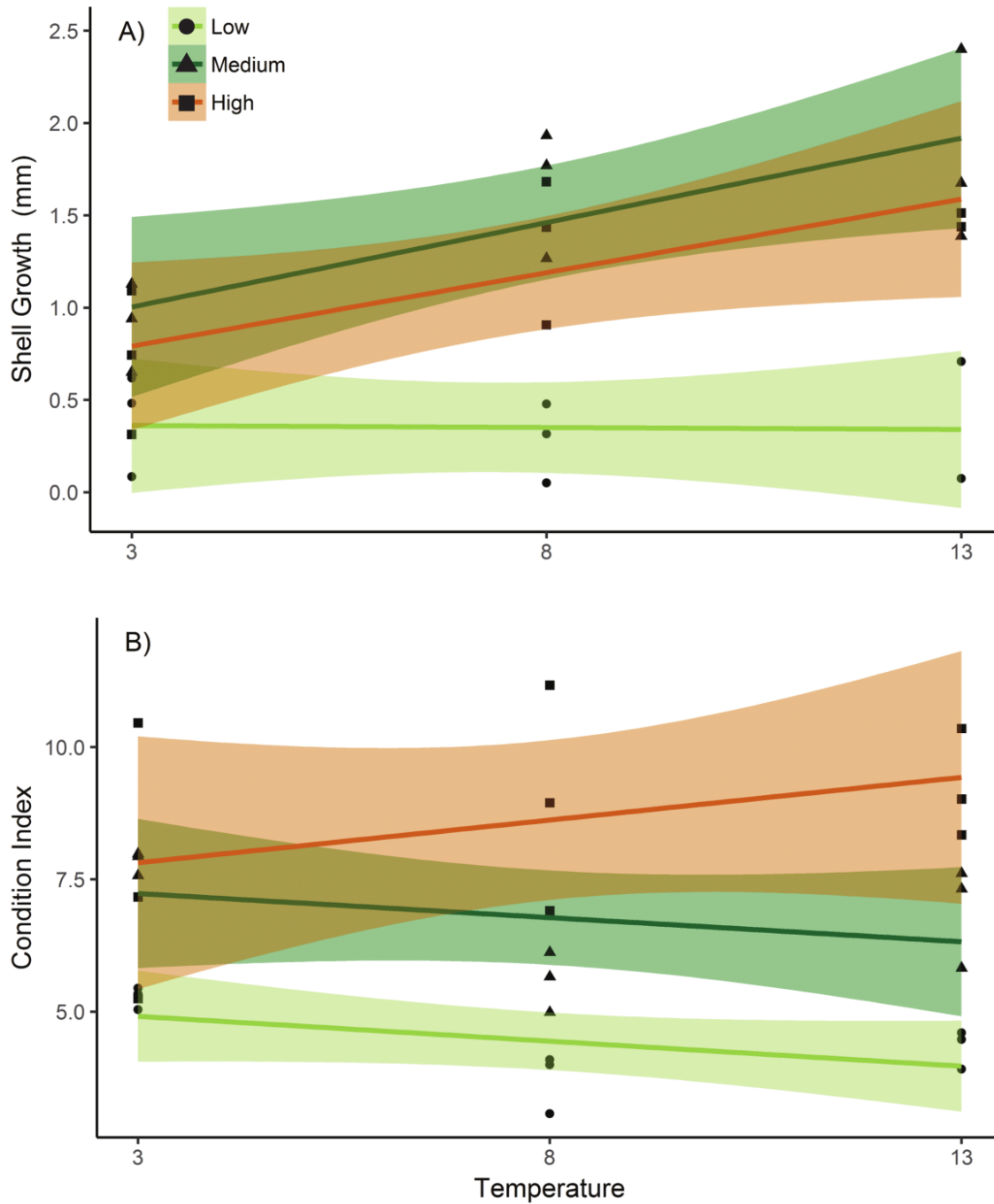
258 During the experiment, water temperature and salinity were constant in the different treatments of
259 the experiment (Table 1). The concentration of phytoplankton cells, however, decreased with
260 temperature (at the same food level). For instance, despite equal supply to the different
261 temperature treatments, the average phytoplankton cells concentration at medium food level,
262 varied from 6.19 (cells/L x 10⁶) at 3 °C to 1.53 at 13 °C (Table 1).

263 The average shell growth increased with increasing food supply, from 0.28 to 1.82 mm in 14
264 weeks (3µm/day - 19µm/day; Table 1, Fig. 2A). At the lowest food level, shell growth was not
265 affected by temperature, but temperature had a positive effect at medium and high food levels
266 (Fig. 2A; Table 2). The condition index was not affected by temperature, but showed an increase
267 with increasing food level (Fig. 2B; Table 2).

268

269 *3.2. Sodium*

270 In the different treatments, the average Na/Ca ranged between 23.27 and 25.98 mmol/mol (Table
271 1; Fig. 3A, B, C). The correlation matrix in Table 3 suggests that the average Na/Ca in the newly
272 deposited carbonate is inversely related to temperature ($r = -0.38$) and positively related to food
273 level ($r = 0.42$). Shell growth at 3 and 8 °C showed higher Na/Ca values ($p = 0.07$; Table 2; Fig.
274 3A, B, C) with higher amounts of supplied food. Only at 13° C, the trend was not clear (Fig. 3C).
275 When the Pearson coefficients were analyzed both food level and temperature showed a
276 significant correlation with Na/Ca values ($r = 0.42$ and $r = -0.38$ respectively, $p < 0.05$; Table 3).
277 At increasing food levels, *A. islandica* shells showed higher Na/Ca values ($p = 0.07$; Table 2; Fig.
278 3A, B, C). Only at 13° C, the trend was not clear (Fig. 3C).

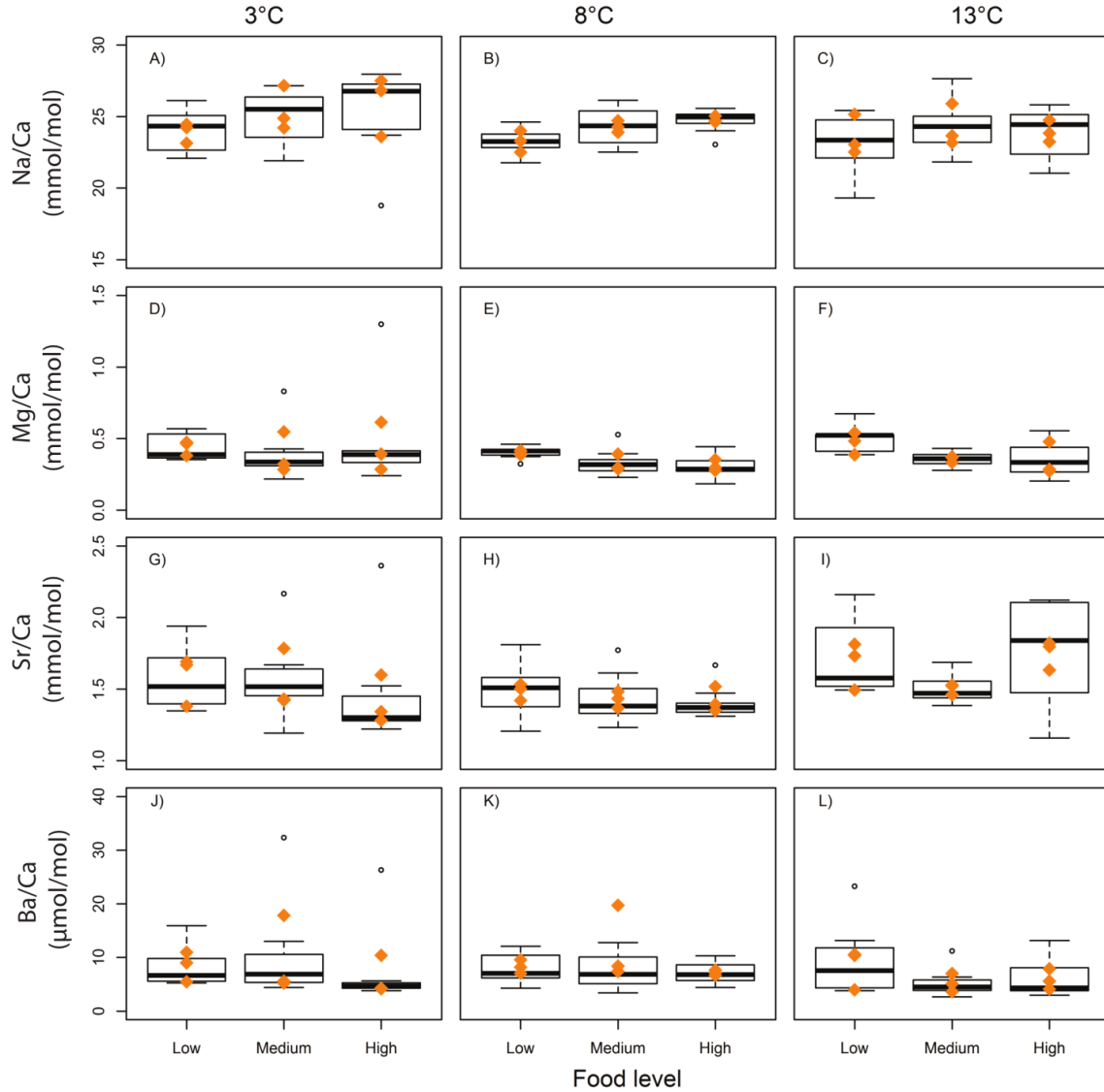


279
 280
 281 **Fig. 2:** Linear regression of the A) average shell growth and B) average condition index of
 282 *Arctica islandica* by treatment (3 temperature x 3 food level x 3 replicates = 27 observations).
 283 Shadow colors show confident intervals. Circle = low food, triangle = medium food, square =
 284 high food.

285 We calculated a linear multiple regression model ($n = 73$ observations) for Na/Ca ratios as a
 286 function of the supplied food, temperature, electrical conductivity (EC), and shell growth to
 287 identify whether external and internal factor(s) are linked to the incorporation of sodium into the
 288 shell carbonate. Na/Ca values are best explained by a combination of shell growth rate and
 289 temperature (Table 4, $p < 0.05$; Fig. 4A, B, C, D). A 32% of the variability in the Na/Ca
 290 (adjusted- $R^2 = 0.316$) was explained by these two factors (correlation between these factors was
 291 0.3). Although a univariate regression model suggested that Na and Condition Index (CI) were
 292 significantly correlated ($r = 0.41$; Table 3), CI was not included in the multiple regression model
 293 because this variable is directly related to shell growth.

	Temp	Food	Na/Ca	log(Mg/Ca)	Sr/Ca	log(Ba/Ca)	GH	CI
Temp		1	0.0487	0.6237	0.0727	0.3799	0.0392	0.9392
Food	0.00		0.0289	0.0384	0.4662	0.1989	0.0100	0.0000
Na/Ca	-0.38	0.42		0.0079	0.0013	0.0017	0.0982	0.0343
log(Mg/Ca)	-0.10	-0.40	-0.50		0.0043	0.0099	0.0011	0.0138
Sr/Ca	0.35	-0.15	-0.59	0.53		0.0694	0.1701	0.9619
log(Ba/Ca)	-0.18	-0.26	-0.58	0.49	0.35		0.1469	0.2598
GH	0.41	0.51	0.34	-0.62	-0.28	-0.30		0.0105
CI	-0.02	0.8	0.41	-0.47	-0.01	-0.22	0.50	

294 **Table 3:** Correlation per treatment (27 observations) among the average element-to-Ca ratios in
 295 the shell and food, temperature (Temp), and physiological factors (shell growth in height (GH)
 296 and condition index (CI) at the end of the experiment). The top right part shows the P-values of
 297 the corresponding correlations.



298
 299 **Fig. 3:** Shell trace-element values per treatment. Orange diamonds indicate average per aquarium
 300 (data used for ANOVA analysis) and boxplot showed the inter-specimens variation (n = 73).

301 *3.3. Magnesium*

302 The average Mg/Ca of *A. islandica* varied between 0.31 and 0.47 mmol/mol (Table 1; Fig. 3D, E,
 303 F). The Mg/Ca correlated inverse but significantly with food level ($r = -0.40$ $p < 0.05$) and CI ($r =$
 304 -0.47 , $p < 0.05$; Table 3) but in a two way ANOVA neither the temperature, food level nor the

305 interaction between these two factors showed statistically significant effects on the average
306 Mg/Ca (Two-way ANOVA, $p > 0.05$; Table 2). The linear multiple regression model however
307 identified shell growth rate as the most likely factor to explain the variation in Mg/Ca ratios
308 between shells (adjusted- $R^2 = 0.234$, Table 4; Fig. 4E, F, G, H).

309

310 *3.4. Strontium*

311 Sr/Ca varied between 1.41 and 1.75 mmol/mol in the freshly grown shell material among the
312 different treatments (Table 1; Fig. 3G, H, I). The Sr/Ca ratio only showed a weak correlation with
313 temperature and had a Pearson correlation coefficient of $r = 0.35$ ($p = 0.07$; Table 3). The
314 correlation with other factors (food level, condition index and shell growth) were insignificant. In
315 the two way ANOVA (to test the effect of temperature, food and their interaction) only
316 temperature showed a statistically significant effect on Sr/Ca (two-way ANOVA, $p \leq 0.05$; Table
317 2). The Sr-trend was negative between 3 and 8 °C but positive if we considered the entire
318 temperature range (between 3-13° C), i.e., levels of Sr were lowest in shells grown at 8 °C.

319 When the role of external and internal factors were considered in a multiple regression model,
320 the stepwise variable selection procedure included the variables growth rate and temperature
321 (adjusted- $R^2 = 15\%$, Table 4; Fig. 4I, J, K, L). Therefore, not only temperature, but also shell
322 growth rate were statistically linked to Sr/Ca.

323

324 *3.5. Barium*

325 Ba/Ca ratios varied greatly among specimens of the same and different treatments. Mean values
326 ranged from 5.26 to 11.84 $\mu\text{mol/mol}$ (Table 1; Fig. 3J, K, L). However, some specimens had

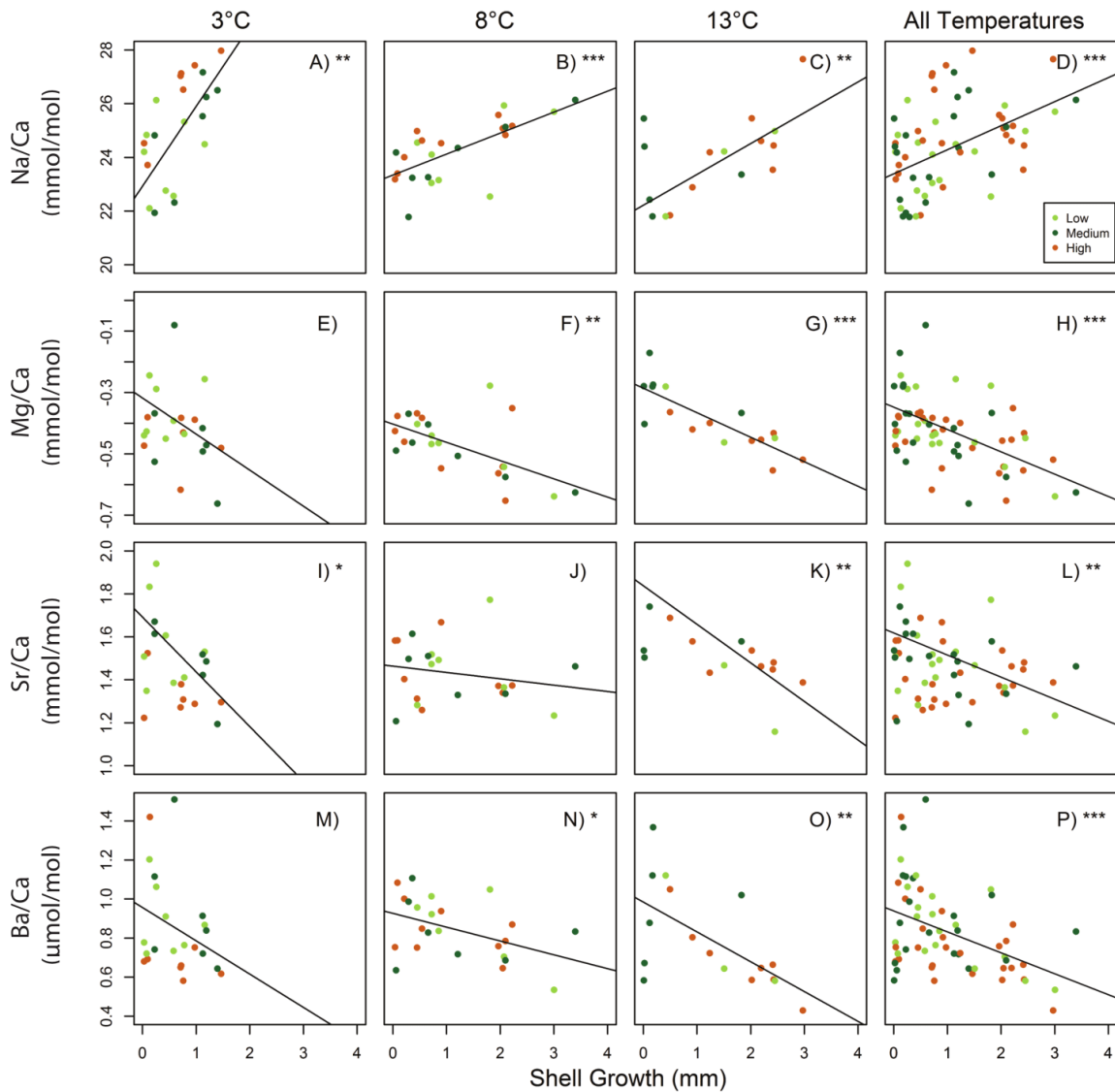
327 peaks higher than 20 $\mu\text{mol/mol}$ (Fig. 3J, K, L). Temperature, food level and the interaction
 328 between these factors did not have a statistically significant effect on Ba/Ca (Two-way ANOVA,
 329 $p > 0.05$; Table 2). When external and internal factors were considered in a multiple regression
 330 model, only shell growth rate was significantly linked to Ba/Ca (adjusted- $R^2 = 0.229$, Table 4;
 331 Fig. 4M, N, O, P).

332

Model	Variables	R ² -adjusted	F-statistic
M_Na	Na ~ <i>Temperature</i> + Food + <i>GH</i> + EC	0.303	7.85
	Na ~ <i>Temperature</i> + <i>GH</i>	0.316	15.57
	Na ~ <i>GH</i>	0.173	14.19
	Na ~ <i>Temperature</i>	0.035	3.58
M_Mg	Log(Mg) ~ <i>Temperature</i> + Food + <i>GH</i> + EC	0.217	5.36
	Log(Mg) ~ <i>Temperature</i> + <i>GH</i>	0.235	10.71
	Log(Mg) ~ <i>GH</i>	0.228	19.70
	Log(Mg) ~ <i>Temperature</i>	0.000	0.46
M_Sr	Sr ~ <i>Temperature</i> + Food + <i>GH</i> + EC	0.125	3.25
	Sr ~ <i>Temperature</i> + <i>GH</i>	0.149	6.52
	Sr ~ <i>GH</i>	0.116	9.24
	Sr ~ <i>Temperature</i>	0.026	2.88
M_Ba	Log(Ba) ~ <i>Temperature</i> + Food + <i>GH</i> + EC	0.144	3.64
	Log(Ba) ~ <i>Temperature</i> + <i>GH</i>	0.236	10.71
	Log(Ba) ~ <i>GH</i>	0.229	19.70
	Log(Ba) ~ <i>Temperature</i>	0.000	0.46

333 **Table 4:** Regression models for each trace element ratio with the significant effect variable highlighted in
 334 italic ($p < 0.05$). Stepwise selection (both directions) selected the model highlighted in bold for each
 335 element ($n=73$, 73 specimens). EC =electric conductivity ($\mu\text{S/cm}$) and GH = shell growth in height.

336



337
 338 **Fig. 4:** Linear relationships between trace element ratios and shell growth in height (73
 339 observations). Dot colors indicate the different food levels: low (light green), medium (dark
 340 green) or high (orange). Statistically significant relationships are expressed as: ‘***’ ($p < 0.001$)
 341 ‘**’ ($p < 0.01$) ‘*’ ($p < 0.05$).

342

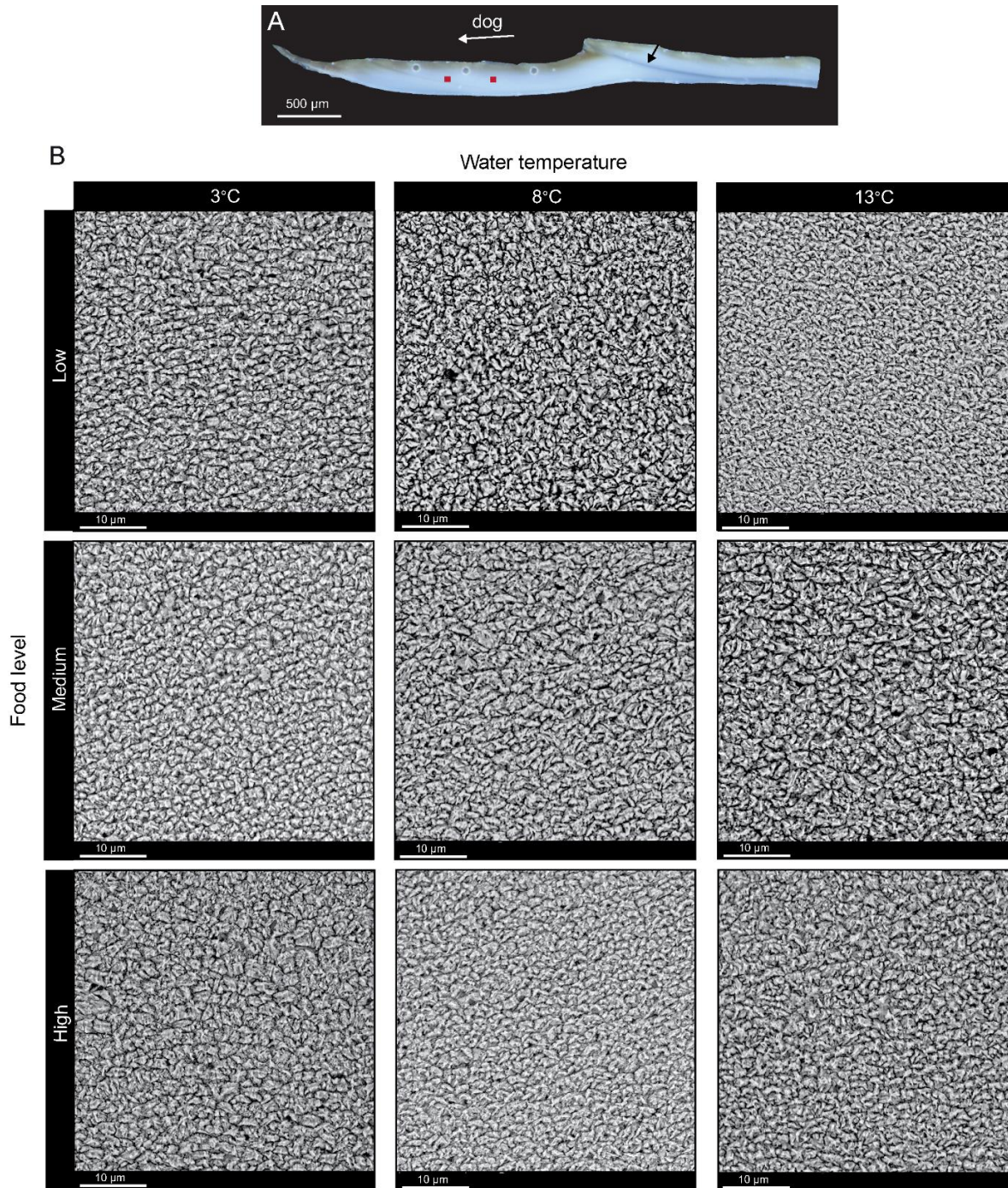
343

344 In summary, shell carbonates that had been formed at lowest food concentration, leading to the
345 lowest shell growth rates, usually incorporated the highest amounts of Mg, Sr and Ba in the shell.
346 Only for Na the opposite was found (Fig. 3, Table 1). All trace element-to-calcium ratios were
347 statistically significantly linked to shell growth rate (Fig. 4; Table 4). Moreover, the Na levels in
348 the shell were also linked to food level and temperature, but Mg only to food, and Sr to temperature.
349 None of the external factors studied (temperature, food, or EC) showed a significant influence on
350 the incorporation of Ba into *A. islandica* shell material grown during this experiment.

351

352 3.6. Microstructure

353 The morphology of the shell microstructures did not significantly vary in relation to the different
354 temperatures and food levels (Fig. 5). In the shells grown at 3 °C, the structural units were
355 characterized by a bulky appearance with no considerable difference between specimens grown at
356 food levels "low" and "medium" (Fig. 5B). Shells growth at the highest food level showed a slight
357 increase in the size of individual biomineral units (Fig. 5B). A similar increase in biomineral unit
358 size was observed in shells reared at 13 °C and medium food level. A minor shift toward more
359 elongated microstructural units was visible in shells exposed to a water temperature of 8 °C and
360 medium food level (Fig. 5B). The most significant morphological difference in shell microstructure
361 was detected in shells grown at 13 °C and low food and in shells reared at 8 °C and high food (Fig.
362 5B). In these cases, the microstructures resembled a well-pronounced crossed-acicular appearance
363 commonly found in the ISL. However, this microstructural variation was not shared by all shells
364 grown at the same treatment. Therefore, on basis of SEM we could not detect a significant variation
365 of *A. islandica* shell microstructures reared at different temperatures and food levels.



366
 367 **Fig. 5:** Microstructural organization of *A. islandica* reared in different environmental conditions.
 368 (A) Shell slab with well visible calcein line marking the start of the experiment (black arrow).
 369 The red squares indicate the approximate location of the SEM images. The three circular spots on
 370 the shell surface are the marks left behind by the LA-ICP-MS measurements. dog = direction of
 371 growth (B) Microstructures formed during the exposure at different water temperatures (3 °C, 8
 372 °C, 13 °C) and food levels (low, medium, and high).

373 **4. Discussion**

374 This study demonstrates that shell growth rate exerts a large control on incorporation of Sr, Mg,
375 Ba and Na into shells (Table 4). The effect of temperature and food on shell chemistry seems
376 overarched by shell growth and varied among the studied elements. Na seems to be affected by a
377 combination of food and temperature, Mg by food, Sr by temperature, and for Ba, we could not
378 demonstrate any effect of food or temperature (Table 3). Therefore, the findings of our study
379 suggest that trace element incorporation into the shell of *A. islandica* is controlled by a complex
380 interplay between environmental and physiological processes. Moreover, the comparison of the
381 microstructural properties of shell growth by SEM could not find external or internal factors
382 affecting *A. islandica* shell microstructural properties.

383

384 *4.1. Controls on trace elemental incorporation into Arctica islandica shells*

385 In many organisms, Sr/Ca and Mg/Ca ratios serve as useful paleo-temperature proxies (e.g.,
386 foraminifera, Nürnberg et al., 1996; corals, Goodkin et al., 2007; sclerosponges, Rosenheim et
387 al., 2004; bivalves, Zhao et al., 2017b). As shown by several studies, in the bivalve *A. islandica*
388 vital effects have an important effect on the incorporation of these two trace elements into the
389 shell (Toland et al., 2000; Foster et al., 2008, 2009; Schöne et al., 2011, 2013; Marali et al.,
390 2017a; Wanamaker and Gillikin, 2018). Most of these studies, which are based on small samples
391 sizes (3-8 specimens vs. 73 this study), concluded that it is unclear whether these metal-to-
392 calcium ratios in the shells of *A. islandica* can be used as temperature proxies. After
393 mathematically eliminating effects of ontogenetic age and growth rate, Schöne et al., (2011)
394 found a significant negative correlation between temperature and Sr/Ca and Mg/Ca ratios
395 (explaining 41 and 27 % of the variability, respectively). In our controlled laboratory study, the

396 amount of Sr incorporated into *A. islandica* was, however, positively and significantly ($r = 0.35$;
397 $p < 0.05$; Table 3) correlated to seawater temperature (Table 2, 3). The difference between both
398 studies could be due to the fact that we used juveniles and not adults, that the specimens came
399 from different populations (Baltic Sea vs. Iceland), or to the small sample size analyzed by
400 Schöne et al., (2011). Hart and Bluzstajn (1998) found, as in this study, a positive relationship
401 between Sr/Ca ratios and temperature in *A. islandica*. Similar observations were previously
402 reported for other bivalve species by Lorrain et al., (2005), Gillikin et al., (2005) and Izumida et
403 al., (2011). Because thermodynamics predict a negative correlation between Sr/Ca and
404 temperature in aragonite, our results corroborate the idea that biological processes play a
405 dominant role in the incorporation of Sr in *A. islandica* shells (Gillikin et al, 2005; Izumida et al.,
406 2011), which is supported by the strong negative relation between shell growth and Sr
407 concentration (Fig. 4).

408 In contrast to Sr/Ca, and despite the broad range of temperatures tested in the present study (3
409 to 13 °C), Mg/Ca was significantly correlated to food level ($r=-0.40$), shell growth ($r=-0.62$) and
410 CI ($r=-0.67$) rather than temperature (Table 3; Fig. 4E, F, G, H). Moreover, multiple regression
411 analysis showed that shell growth rate explained 23 % of the Mg/Ca variability, and identified the
412 effect of temperature as being negligible in our data set (Table 4). Thus, it appears that the Sr/Ca
413 and Mg /Ca ratios of *A. islandica* shells to a large proportion reflect physiological processes and
414 do not exclusively reflect water temperature (Gillikin et al., 2005; Freitas et al., 2006; Elliot et al.,
415 2009; Foster et al., 2008, 2009; Wanamaker et al., 2008; Geeza et al., 2018; Wanamaker and
416 Gillikin, 2018).

417 Although Ba/Ca ratios in some marine bivalves are used as proxy for paleo-productivity (e.g.,
418 Stecher et al., 1996; Vander Putten et al., 2000; Gillikin et al., 2008; Thébault et al., 2009; Hatch

419 et al., 2013), we could not find a clear relationship between Ba/Ca ratios of our experimental *A.*
420 *islandica* shells and food availability. The results however again suggest that Ba levels were related
421 to shell growth rate, which could explain 23% of the variability in the shell Ba concentration,
422 comparable to what has been found for the freshwater pearl mussel *Hyriopsis* sp. (Izumida et al.,
423 2011). The large Ba peaks detected in some of our specimens did not show any pattern in
424 relationship to the food concentration where those bivalves grew, instead we observed strong Ba/Ca
425 peaks even at the lowest food level (Fig. 3J, K, L). Moreover, not all specimens from the same
426 aquarium (or same treatment) showed large Ba peaks, as it was previously reported about wild
427 populations of *A. islandica* (Gillikin et al., 2008; Marali et al., 2017a, b). Although we kept the
428 food concentration constant (per treatment) over the entire experimental period, and the food used
429 was chemically homogenous, slight variations in the food supply could be the reason for the
430 asynchrony of Ba peaks between individuals. Additionally, the time lag between feeding and
431 incorporation of Ba into the shell, i.e., the moment that the animals really deposited their shell, can
432 differ between specimens and these differences can be more evident in studies of short-period of
433 time such as ours (experimental period =14 weeks). Moreover, since different specimens had
434 different shell growth rates the laser spots made to sublimate the carbonate might have reflected
435 different periods or period lengths and thus have led to different sampled time frames or time
436 frames with different time resolution (this could apply to all trace-elements analyzed). To get better
437 insight about the timing of Ba peaks, constant series of laser spots should have been done over all
438 the newly formed shell. Therefore, even though we did not find synchrony in the Ba peaks among
439 specimens, we cannot exclude it either.

440 Interestingly, Na/Ca of *A. islandica* exhibited a significant correlation with food ($r = 0.42$)
441 and temperature ($r = -0.38$; Table 3). When several different external and internal factors were

442 simultaneously considered in a multiple regression model, shell growth and temperature explained
443 about 1/3 of the variability of Na/Ca (adjusted-R² = 32 %, Table 4). Since salinity was kept stable
444 during the course of the experiment (indicating that variation of Na/Ca ratio in the water was small),
445 water chemistry interference on Na/Ca variations are unlikely (Table 2, 4). A possible explanation
446 for the observed correlation between food and Na/Ca or temperature and Na/Ca (Table 3) could be
447 that Na/Ca reflects the metabolic rate of *A. islandica*, with the latter being strongly affected by
448 temperature and food supply (Winter 1978). Support for such an interpretation comes from the
449 finding that the condition index was also significantly correlated with Na/Ca ($r = 0.41$; $p < 0.05$).
450 Zhao et al., (2017a) demonstrated that Na/Ca is related to the acid-base and ionic regulation in the
451 calcifying fluid of *Mytilus edulis* shells, a process strongly linked to biomineralisation and highly
452 dependent on the metabolic activity. Hence, when the change of Na/Ca_{water} is small, physiological
453 influences may exert a major control on the incorporation of Na into bivalve shells.

454 Our findings seem to indicate that, under food limitation, *A. islandica* is less efficient in
455 discriminating against trace and minor element impurities of the carbonate matrix and that
456 physiological processes play an important role in the control on elemental incorporation into *A.*
457 *islandica* shells.

458

459 4.2. Controls on microstructural characteristics of *A. islandica* shells

460 According to the results of the present study, the shell microstructure of *Arctica islandica* was not
461 significantly affected by water temperature or dietary regimes. Although some slight differences
462 were visible among the treatments (i.e., biomineral size increase and shape variation), the lack of
463 consistency of these specific alterations suggest that the observed differences may not be related to

464 the two studied environmental variables. The small morphological variability may be explained by
465 differences among specimens. Our observations are in good agreement with Milano et al., (2017a)
466 which results also indicated that the morphology of biomineral units in *A. islandica* shells is not
467 influenced by water temperature or diet. Note that in their study, the role of these two
468 environmental factors on crystal morphology were investigated in separate experiments whereas
469 we went further in the current research by studying the effect of both environmental variables in
470 one experiment. We did not find, however, an interaction effect on crystal morphology, size, or
471 orientation at the temperature and food conditions considered.

472 Previously, microstructures of other mollusk species were shown to be influenced by the
473 environment (Hedegaard et al., 2006; Nehrke and Nouet, 2011; Soldatov et al., 2013; Stemmer
474 and Nehrke, 2014; Milano et al., 2017a). For instance, water temperature was identified as the
475 major factor controlling size and shape of individual biomineral units in the non-denticular
476 composite prismatic microstructure of *Cerastoderma edule* (Milano et al., 2017b). Similarly, the
477 relative thickness of the composite prismatic layer of *Scapharca broughtonii* was shown to be
478 negatively correlated with water temperature in naturally and laboratory-based grown specimens
479 (Nishida et al., 2012, 2015). In these species, the sensitivity of the shell microstructure to
480 environmental fluctuations, especially temperature, offers the potential to use microstructural
481 properties as environmental proxies. However, the possibility of using shell architecture for
482 paleoenvironmental reconstructions largely depends on the type of microstructure considered, the
483 species under study, and the methodology applied (Nishida et al., 2012; Milano et al., 2017 b;
484 Purroy et al., 2018). Among the different mollusk species, microstructures are highly diversified,
485 coming with different morphometric and mineralogical properties (Nishida et al., 2012; Milano et
486 al., 2017 b). In the case of homogenous microstructures as in *A. islandica*, the lack of a specific
487 alignment among the biomineral units together with their irregular shape, challenges the

488 identification of potential structural changes. Unlike prismatic and crossed-lamellar structures,
489 where variations in morphometric and alignment parameters can be easily detected using SEM, *A.*
490 *islandica* microstructures may require assessments on the crystallophic properties, more than from
491 the morphometric ones (Milano et al., 2017a).

492

493 **5. Conclusions**

494 Factors influencing the incorporation of trace elements into biogenetic carbonates are complex
495 (Stecher et al., 1996) and species-specific (Gillikin et al., 2005; Freitas et al., 2006; Zhao et al.,
496 2017b). Although element-to-calcium ratios in *A. islandica* shells contain environmental
497 information, this information cannot be easily distinguished from physiological controls (mainly
498 shell growth rate). Specifically, the pathways of elements from the water and food into the shell
499 needs further study. Our study, however, supports the conclusion of Wanamaker and Gillikin
500 (2018) that at present, there is not yet enough and consistent information that would allow to use
501 trace element-to-calcium ratios of *A. islandica* shells as reliable environmental proxies.

502 With the SEM technique used in this study, we could not find a significant variation in the
503 morphometric characteristics of *A. islandica* microstructures relating on the studied
504 environmental variables (i.e. temperature and food). We think, however, that subsequent studies
505 with different and more advanced methods (for instance: Confocal Raman Microscopy and
506 Electron Backscatter Diffraction; Milano et al., 2017a) can identify physical properties of
507 microstructures as proxies for paleoenvironmental reconstructions.

508

509

510

511 **Acknowledgments**

512 We thanks the Alfred-Wegener-Institute (AWI) for its collaboration and especially to Cyril
513 Degletagne and Doris Abele for providing the specimens used in this study. This work was
514 funded by the EU within the framework (FP7) of the Marie Curie International
515 Training Network ARAMACC (604802).

516 The study data is available at doi:10.4121/uuid:bd1c80a5-1bd2-426a-a9d7-97ce67446886.

517

518 **References**

- 519 Abele et al., 2009. Bivalve models of aging and the determination of molluscan lifespans. *Exp.*
520 *gerontol.* 44: 307–315. doi: 10.1016/j.exger.2009.02.012
- 521 Ambrose et al., 2012. Growth line deposition and variability in growth of two circumpolar
522 bivalves (*Serripes groenlandicus*, and *Clinocardium ciliatum*). *Polar Biol.* 35: 345–354. doi:
523 10.1007/s00300-011-1080-4
- 524 Ballesta-Artero et al., 2018. Interactive effects of temperature and food availability on the growth
525 of *Arctica islandica* (Bivalvia) juveniles. *Mar. Environ. Res.* 133:67–77. doi:
526 10.1016/j.marenvres.2017.12.004
- 527 Butler et al., 2013. Variability of marine climate on the North Icelandic Shelf in a 1357-year proxy
528 archive based on growth increments in the bivalve *Arctica islandica*. *Palaeogeogr*
529 *Palaeoclimatol Palaeoecol* 373:141–151. doi:10.1016/j.palaeo.2012.01.016
- 530 Carter et al., 2012. Illustrated glossary of the Bivalvia. *Treatise Online*: 1-209.
- 531 Dodd, 1965. Environmental control of strontium and magnesium in *Mytilus*. *Geochim. Gosmochim.*
532 *Acta.* 29: 385–398. doi: 10.1016/0016-7037(65)90035-9
- 533 Dunca et al., 2009. Using ocean quahog (*Arctica islandica*) shells to reconstruct palaeoenvironment
534 in Öresund, Kattegat and Skagerrak, Sweden. *Int J Earth Sci* 98:3–17. doi:10.1007/s00531-
535 008-0348-6
- 536 Duncan, 2011. Healthcare risk adjustment and predictive modeling. Actex Publications.

537 Elliot et al., 2009. Profiles of trace elements and stable isotopes derived from giant long-lived
538 *Tridacna gigas* bivalves: potential applications in paleoclimate studies. *Palaeogeogr.*
539 *Palaeoclimatol. Palaeoecol.* 280: 132–142. doi: 10.1016/j.palaeo.2009.06.007

540 Foster et al., 2009. Strontium distribution in the shell of the aragonite bivalve *Arctica islandica*.
541 *Geochem. Geophys. Geosyst.* 10(3). doi: 10.1029/2007GC001915

542 Foster et al., 2008. Mg in aragonitic bivalve shells: Seasonal variations and mode of incorporation
543 in *Arctica islandica*. *Chem. Geol.* 254: 113–119. doi: /10.1016/j.chemgeo.2008.06.007

544 Freitas et al., 2006. Environmental and biological controls on elemental (Mg/Ca, Sr/Ca and Mn/Ca)
545 ratios in shells of the king scallop *Pecten maximus*. *Geochim. Gosmochim. Acta.* 70: 5119–
546 5133. doi: 10.1016/j.gca.2006.07.029

547 Freitas et al., 2005. Mg/Ca, Sr/Ca, and stable-isotope ($\delta^{18}\text{O}$ and $\delta^{13}\text{C}$) ratio profiles from the fan
548 mussel *Pinna nobilis*: Seasonal records and temperature relationships. *Geochem. Geophys.*
549 *Geosyst.* 6(4). doi: 10.1029/2004GC000872

550 Geeza, et al., 2018. Controls on magnesium, manganese, strontium, and barium concentrations
551 recorded in freshwater mussel shells from Ohio. *Chem. Geol.* doi:
552 10.1016/j.chemgeo.2018.01.001

553 Gillikin et al., 2008. Synchronous barium peaks in high-resolution profiles of calcite and aragonite
554 marine bivalve shells. *Geo-Mar. Lett.* 28: 351–358. doi: 10.1007/s00367-008-0111-9

555 Gillikin et al., 2006. Barium uptake into the shells of the common mussel (*Mytilus edulis*) and the
556 potential for estuarine paleo-chemistry reconstruction. *Geochim. Gosmochim. Acta.* 70: 395–
557 407. doi: 10.1016/j.gca.2005.09.015

558 Gillikin et al., 2005. Strong biological controls on Sr/Ca ratios in aragonitic marine bivalve shells.
559 *Geochem. Gosmochim. Acta.* 6 (5). doi: 10.1029/2004GC000874

560 Goodkin et al., 2007. A multicoral calibration method to approximate a universal equation relating
561 Sr/Ca and growth rate to sea surface temperature. *Paleoceanography* 22. doi:
562 10.1029/2006PA001312

563 Graham, 2003. Confronting multicollinearity in ecological multiple regression. *Ecology* 84:2809–
564 2815. doi:10.1890/02-3114

565 Hart and Blusztajn, 1998. Clams as recorders of ocean ridge volcanism and hydrothermal vent field
566 activity. *Science* 280: 883–886. doi: 10.1126/science.280.5365.883

567 Hatch et al., 2013. Ba/Ca variations in the modern intertidal bean clam *Donax gouldii*: An
568 upwelling proxy. *Palaeogeogr. Palaeoclimatol. Palaeoecol.* 373: 98–107. doi:
569 10.1016/j.palaeo.2012.03.006

570 Hedegaard et al., 2006. Molluscan shell pigments: An in situ resonance Raman study, *J. Mollus.*
571 *Stud.* 72: 157–162. doi:10.1093/mollus/eyi062

572 Ieno and Zuur, 2015. A beginner's guide to data exploration and visualization with R. Highland
573 Statistics Ltd., Newburgh, United Kingdom

574 Izumida et al., 2011. Biological and water chemistry controls on Sr/Ca, Ba/Ca, Mg/Ca and $\delta^{18}\text{O}$
575 profiles in freshwater pearl mussel *Hyriopsis* sp. *Palaeogeogr. Palaeoclimatol. Palaeoecol.* 309:
576 298–308. doi: 10.1016/j.palaeo.2011.06.014

577 Jochum et al., 2012. Accurate trace element analysis of speleothems and biogenic calcium
578 carbonates by LA-ICP-MS. *Chem. Geol.* 318-319, 31-44. doi:
579 10.1016/j.chemgeo.2012.05.009

580 Jochum et al., 2011. Determination of reference values for NIST SRM 610-617 glasses following
581 ISO guidelines. *Geostand. Geoanal. Res.* 35: 397-429. doi: 10.1111/j.1751-
582 908X.2011.00120.x

583 Jochum, et al., 2005. GeoReM: a new geochemical database for reference materials and isotopic
584 standards. *Geostand. Geoanal. Res.* 29: 87-133. doi: 10.1111/j.1751-908X.2005.tb00904.x

585 Klein et al., 1996. Sr/Ca and $^{13}\text{C}/^{12}\text{C}$ ratios in skeletal calcite of *Mytilus trossulus*: Covariation with
586 metabolic rate, salinity, and carbon isotopic composition of seawater. *Geochim. Cosmochim.*
587 *Acta.* 60: 4207–4221. doi: 10.1016/S0016-7037(96)00232-3

588 Klünder et al., 2008. Laser ablation analysis of bivalve shells – archives of environmental
589 information. *Geol. Surv. Denm. Greenl. Bull.* 15: 89–92.

590 Linard et al., 2011. Calcein staining of calcified structures in pearl oyster *Pinctada margaritifera*
591 and the effect of food resource level on shell growth. *Aquaculture* 313: 149–155.
592 doi:10.1016/j.aquaculture.2011.01.008

593 Lorens and Bender, 1980. The impact of solution chemistry on *Mytilus edulis* calcite and aragonite.
594 *Geochim. Cosmochim. Acta.* 44: 1265–1278. doi: 10.1016/0016-7037(80)90087-3

595 Lorrain et al., 2005. Strong kinetic effects on Sr/Ca ratios in the calcitic bivalve *Pecten maximus*.
596 *Geology* 33: 965–968. doi: doi.org/10.1130/G22048.1

597 Lutz, 1984. Paleocological implications of environmentally controlled variation in molluscan
598 shell microstructure, *Geobios* 17: 93–99. doi:10.1016/S0016-6995(84)80161-8

599 Marali et al., 2017a. Reproducibility of trace element time-series (Na/Ca, Mg/Ca, Mn/Ca, Sr/Ca,
600 and Ba/Ca) within and between specimens of the bivalve *Arctica islandica*—A LA-ICP-MS line
601 scan study. *Palaeogeogr. Palaeoclimatol. Palaeoecol.* 484: 109–128. doi:
602 10.1016/j.palaeo.2016.11.024

603 Marali, et al., 2017b. Ba/Ca ratios in shells of *Arctica islandica*—Potential environmental proxy
604 and crossdating tool. *Palaeogeogr. Palaeoclimatol. Palaeoecol.* 465: 347–361. doi:
605 10.1016/j.palaeo.2015.12.018

606 Milano et al., 2017a. The effects of environment on *Arctica islandica* shell formation and
607 architecture. *Biogeosciences* 14: 1577–1591. doi:10.5194/bg-14-1577-2017

608 Milano et al., 2017b. Changes of shell microstructural characteristics of *Cerastoderma edule*
609 (*Bivalvia*) - A novel proxy for water temperature. *Palaeogeogr. Palaeoclimatol. Palaeoecol.* 465:
610 395–406. doi:10.1016/j.palaeo.2015.09.051

611 Nehrke and Nouet, 2011. Confocal Raman microscope mapping as a tool to describe different
612 mineral and organic phases at high spatial resolution within marine biogenic carbonates: case
613 study on *Nerita undata* (Gastropoda, Neritopsina). *Biogeosciences* 8: 3761–3769.
614 doi:10.5194/bg-8-3761-2011

615 Nishida et al., 2015. Thermal dependency of shell growth, microstructure, and stable isotopes in
616 laboratory-reared *Scapharca broughtonii* (Mollusca: Bivalvia). *Geochem. Geophys.*
617 *Geosystems* 16: 2395–2408. doi:10.1002/2014GC005684

618 Nishida et al., 2012. Seasonal changes in the shell microstructure of the bloody clam, *Scapharca*
619 *broughtonii* (Mollusca: Bivalvia: Arcidae). *Palaeogeogr. Palaeoclimatol. Palaeoecol.* 363–364,
620 99–108. doi:10.1016/j.palaeo.2012.08.017

621 Nürnberg et al., 1996. Assessing the reliability of magnesium in foraminiferal calcite as a proxy
622 for water mass temperatures. *Geochim. Cosmochim. Acta.*, 60: 803–814. doi: 10.1016/0016-
623 7037(95)00446-7

624 O'Neil and Gillikin, 2014. Do freshwater mussel shells record road-salt pollution? *Sci. Rep.* 4: 7168.
625 doi: 10.1038/srep07168

626 Poulain et al., 2015. An evaluation of Mg/Ca, Sr/Ca, and Ba/Ca ratios as environmental proxies in
627 aragonite bivalve shells. *Chem. Geol.* 396: 42–50. doi: 10.1016/j.chemgeo.2014.12.019

628 Purroy et al., 2018. Drivers of shell growth of the bivalve, *Callista chione* (L. 1758)—Combined
629 environmental and biological factors. *Mar. Environ. Res.* 134:138–149. doi:
630 10.1016/j.marenvres.2018.01.011

631 Purton et al., 1999. Metabolism controls Sr/Ca ratios in fossil aragonitic mollusks. *Geology* 27:
632 1083–1086. doi: 10.1130/0091-7613(1999)027%3C1083:MCSCRI%3E2.3.CO;2

633 Rosenheim et al., 2004. High resolution Sr/Ca records in sclerosponges calibrated to temperature
634 in situ. *Geology* 32: 145–148. doi: 10.1130/G20117.1

635 Rucker and Valentine, 1961. Salinity response of trace element concentration in *Crassostrea*
636 *virginica*. *Nature*, 190: 1099. doi:10.1038/1901099a0

637 Schöne et al., 2013. Crystal fabrics and element impurities (Sr/Ca, Mg/Ca, and Ba/Ca) in shells of
638 *Arctica islandica*—Implications for paleoclimate reconstructions. *Palaeogeogr. Palaeoclimatol.*
639 *Palaeoecol.* 373: 50–59. doi:10.1016/j.palaeo.2011.05.013

640 Schöne et al., 2011. Sr/Ca and Mg/Ca ratios of ontogenetically old, long-lived bivalve shells
641 (*Arctica islandica*) and their function as paleotemperature proxies. *Palaeogeogr.*
642 *Palaeoclimatol. Palaeoecol.* 302: 52–64. doi: 10.1016/j.palaeo.2010.03.016

643 Schöne et al., 2010. Effect of organic matrices on the determination of the trace element chemistry
644 (Mg, Sr, Mg/Ca, Sr/Ca) of aragonitic bivalve shells (*Arctica islandica*)—Comparison of ICP-
645 OES and LA-ICP-MS data. *Geochem. J.* 44: 23–37. doi: 10.2343/geochemj.1.0045

646 Soldatov et al., 2013. Qualitative composition of carotenoids, catalase and superoxide dismutase
647 activities in tissues of bivalve mollusc *Anadara inaequalis* (Bruguiere, 1789), *J. Evol.*
648 *Biochem. Phys.*, 49: 3889–398. doi:10.1134/S0022093013040026

649 Stecher et al., 1996. Profiles of strontium and barium in *Mercenaria mercenaria* and *Spisula*
650 *solidissima* shells. *Geochim. Gosmochim. Acta.* 60: 3445–3456. doi: 10.1016/0016-
651 7037(96)00179-2

652 Stemmer and Nehrke, 2014. The distribution of polyenes in the shell of *Arctica islandica* from
653 North Atlantic localities: a confocal Raman microscopy study. *J. Molluscan Stud.* 80: 365–
654 370, <https://doi.org/10.1093/mollus/eyu033>

655 Strasser et al., 2008. Temperature and salinity effects on elemental uptake in the shells of larval
656 and juvenile softshell clams *Mya arenaria*. Mar. Ecol. Prog. Ser. 370, 155–169. doi:
657 10.3354/meps07658

658 Surge and Walker, 2006. Geochemical variation in microstructural shell layers of the southern
659 quahog (*Mercenaria campechiensis*): Implications for reconstructing seasonality.
660 Palaeogeogr. Palaeoclimatol. Palaeoecol. 237: 182–190. doi: /10.1016/j.palaeo.2005.11.016

661 Tan Tiu, 1988. Temporal and spatial variation of shell microstructure of *Polymesoda caroliniana*
662 (Bivalvia: Heterodonta). Am. Malacol. Bull. 6: 199–206.

663 Tan Tiu and Prezant, 1989. Temporal variation in microstructure of the inner shell surface of
664 *Corbicula fluminea* (Bivalvia: Heterodonta), Am. Malacol. Bull. 7: 65–71.

665 Tan Tiu and Prezant, 1987. Shell microstructural responses of *Geukensia demissa granosissima*
666 (Mollusca: Bivalvia) to continual submergence, Am. Malacol. Bull. 5: 173–176.

667 Thébault et al., 2009. Barium and molybdenum records in bivalve shells: Geochemical proxies for
668 phytoplankton dynamics in coastal environments? Limnol. Oceanogr. 54: 1002–1014. doi:
669 10.4319/lo.2009.54.3.1002

670 Toland et al., 2000. A study of sclerochronology by laser ablation ICP-MS. J. Anal., At.
671 Spectrom. 15: 1143–1148. doi: 10.1039/b002014l

672 Urey et al., 1951. Measurement of paleotemperatures and temperatures of the Upper Cretaceous of
673 England, Denmark, and the southeastern United States. Bull. Geol. Soc. Am. 62: 399–416.
674 doi: 10.1130/0016-7606(1951)62[399:MOPATO]2.0.CO;2

675 Vander Putten et al., 2000. High resolution distribution of trace elements in the calcite shell layer
676 of modern *Mytilus edulis*: Environmental and biological controls. *Geochim. Cosmochim.*
677 *Acta.* 64: 997–1011. doi: 10.1016/S0016-7037(99)00380-4

678 Wanamaker and Gillikin. 2018. Strontium, magnesium, and barium incorporation in aragonitic
679 shells of juvenile *Arctica islandica*: Insights from temperature controlled experiments. *Chem.*
680 *Geol.* doi: 10.1016/j.chemgeo.2018.02.012.

681 Wanamaker et al., 2008. Experimentally determined Mg/Ca and Sr/Ca ratios in juvenile bivalve
682 calcite for *Mytilus edulis*: implications for paleotemperature reconstructions. *Geo-Mar. Lett.*
683 28: 359–368. doi: 10.1007/s00367-008-0112-8

684 Winter, 1978. A review on the knowledge of suspension-feeding in lamellibranchiate bivalves,
685 with special reference to artificial aquaculture systems. *Aquaculture* 13: 1–33. doi:
686 10.1016/0044-8486(78)90124-2.

687 Zhao et al., 2017a. Insights from sodium into the impacts of elevated $p\text{CO}_2$ and temperature on
688 bivalve shell formation. *J. Exp. Mar. Biol. Ecol.* 486: 148–154. doi:
689 10.1016/j.jembe.2016.10.009

690 Zhao et al., 2017b. Controls on strontium and barium incorporation into freshwater bivalve shells
691 (*Corbicula fluminea*). *Palaeogeogr. Palaeoclimatol. Palaeoecol.* 465: 386–394. doi:
692 10.1016/j.palaeo.2015.11.040

693